Electronic Supplementary Material (ESI) for Journal of Materials Chemistry C.

# Dimer with Thermally Activated Delayed Fluorescence (TADF) Emission in Non-Doped Device

Xing Chen,[a] Aziz Khan,[a] Sheng-Nan Zou,[a] Yun Li,[a] Qi-Sheng Tian,[a] Cheng Zhong*[b], Man-Keung Fung*[ac], Zuo-Quan Jiang*[a] and Liang-Sheng Liao[ac]

[a] Jiangsu Key Laboratory for Carbon-Based Functional Materials & Devices, Institute of Functional Nano & Soft Materials (FUNSOM), Soochow University 199 Ren'ai Road, Suzhou, Jiangsu 215123, China
*E-mail:* mkfung@suda.edu.cn, zqjiang@suda.edu.cn

[b] Hubei Key Lab on Organic and Polymeric Optoelectronic Materials, Department of Chemistry, Wuhan University,
299 Bayi Road, Wuhan, 430072, Hubei, P. R. China
*E-mail:* zhongcheng@whu.edu.cn

[c] Macao Institute of Materials Science and Engineering, Macau University of Science and Technology, Taipa, Macau SAR, 999078 P. R. China

# Content

# 1. Experimental Section

## 1.1 Materials and instruments

The raw reagents, catalysts and chemicals involved in the initial reaction were purchased from commercial sources and used without further purification. Tetrahydrofuran (THF), and 1,4-dioxane used in synthetic routes were purified by PURE SOLV (Innovative Technology) purification system. The $^1H$ NMR and $^{13}C$ NMR spectra were measured on Bruker 400 and Bruker 600 spectrometer in deuterated chloroform solvent with trimethylsilane (TMS) as reference. Matrix-Assisted Laser Desorption/ Ionization Time of Flight Mass Spectrometry MS-MALDI (TOF) was performed using a Bruker Autoflex II / Compass 1.0. The ultraviolet−visible (UV−vis) absorption spectra were measured by a Shimadzu UV-2600 spectrophotometer. Fluorescent and phosphorescent spectra were measured by a Hitachi F-4600 and FLUOROMAX-4 spectrophotometer. Thermogravimetric analysis (TGA) was measured by a METTLER TOLEDO TGA1 under high purity nitrogen atmosphere. The temperature was increased to 800 $^oC$ with a heating rate of 10 $^oC$/minute. Electrochemical analysis was achieved on a CHI 600D electrochemical work station, and the scan rate was 100 mV $S^{-1}$ at room temperature. The three-electrode configuration system in $n$-$Bu_4NPF_6$ (0.1 M) $CH_2Cl_2$ solution. The redox potential of ferrocene/ferrocenium ($Fc/Fc^+$) was measured under room temperature (for calibration). The PLQY was measured using Hamamatsu C9920-02G in nitrogen or air atmosphere. Transient spectra were obtained by using the Quantaurus-Tau fluorescence lifetime measurement system (C11367-03, Hamamatsu Photonics Co.) in vacuum or nitrogen atmosphere. Elemental analysis was measured using Vario Micro cube.

## 1.2 Device fabrication process

OLED devices were fabricated on ITO glass substrates (130 nm,15 Ω/sq) under a base pressure of $4\times10^{-6}$ Torr and the active area of the devices was 0.1 $cm^2$. The substrate was ultrasonically cleaned sequentially with acetone, ethanol, and deionized water, and dried in an oven at 120 $^oC$ for 5 h. Then, it was treated with ultraviolet ozone for 15 mins before placing it in a vacuum chamber. All organic materials' deposited rates were

2 Å/s, and Al's is 6-8 Å/s. The deposition rate of the dopant was adjusted according to the volume ratio doped in the host materials. Quartz crystals would monitor all materials' deposition rate and thickness.

The EL information such as EL spectra, current efficiency (CE), power efficiency (PE), CIE coordinate, voltage of device and luminance were all recorded via a programmable spectrum scan photometer (PHOTO RESEARCH, PR 655) and KEITHLEY 2400 source meter. All the measurements were conducted in ambient air at room temperature, and the external quantum efficiency was calculated assuming Lambertian distribution of light emission.

### 1.3 DFT Methods.

All optimizations are finished at PBE0/def2-SVP level with Grimme's D3BJ [1] empirical dispersion correction. The relaxed excited states are optimized at TD-CAM-B3LYP/def2-SVP level with GD3BJ correction. The transition energies are PCM solvation model used with diphenyl ether as solvent. The dielectric constant of diphenyl ether is 3.73, which resemble the environment of organic solids. All the calculations are performed by the Gaussian 09 program and the hole-electron distribution analysis is performed by the Multiwfn program. [2]

# 2. Supporting Figures

## 2.1 Experimental data of synthesis

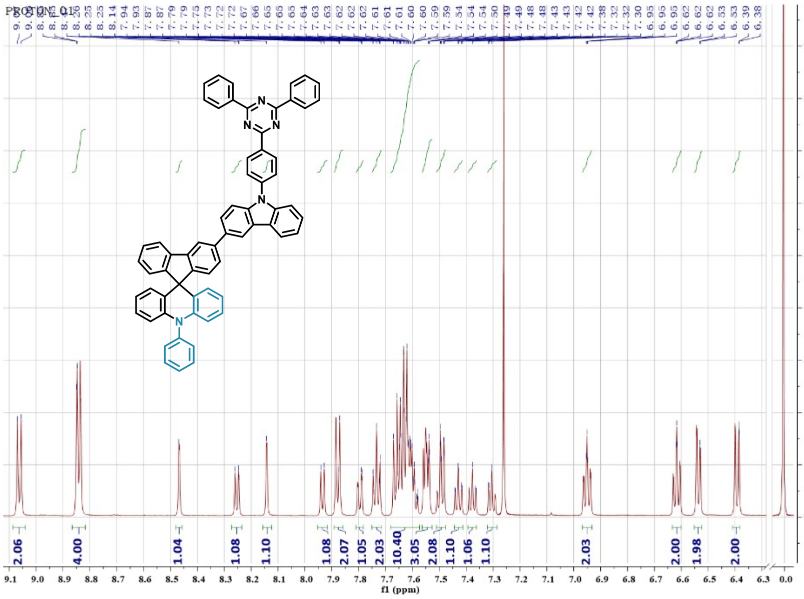

**Figure S1.** 600 MHz $^1$H NMR spectrum of **SFCCN** measured in $CDCl_3$**.**

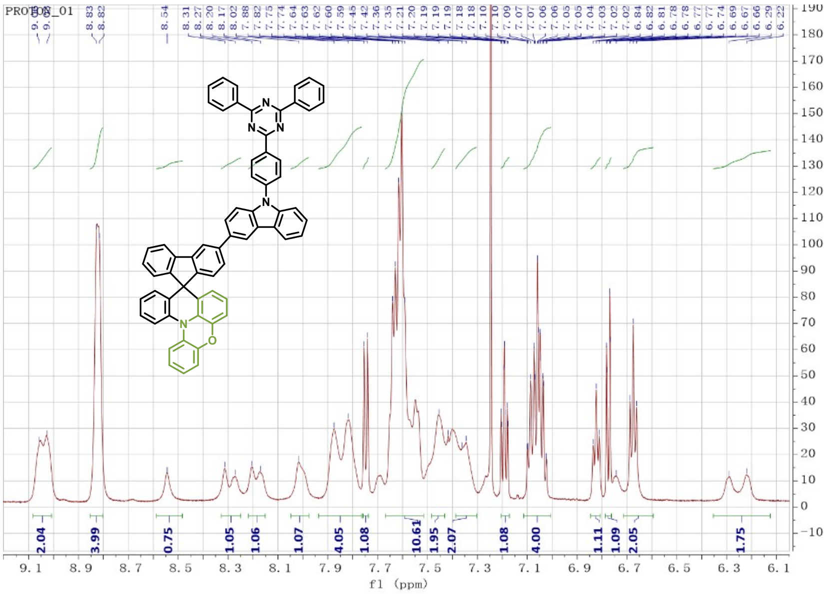

**Figure S2.** 600 MHz $^1$H NMR spectrum of **SFCCNO** measured in $CDCl_3$**.**

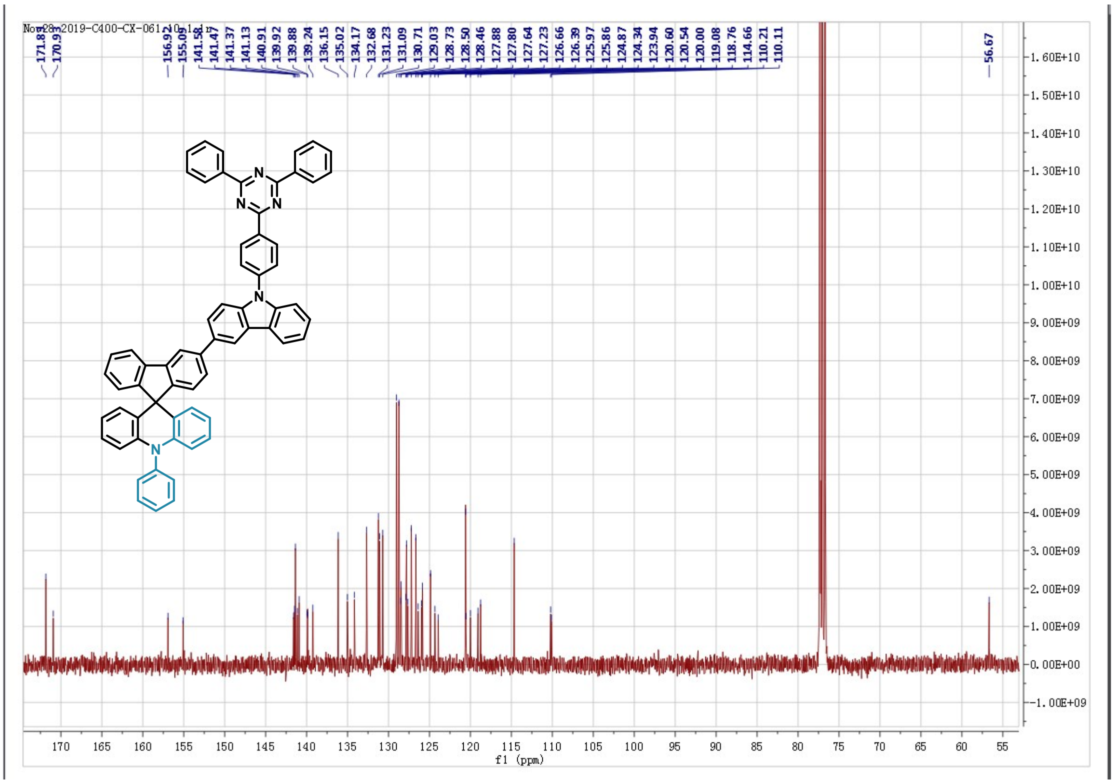

**Figure S3.** 101 MHz $^{13}C$ NMR spectrum of **SFCCN** measured in $CDCl_3$**.**

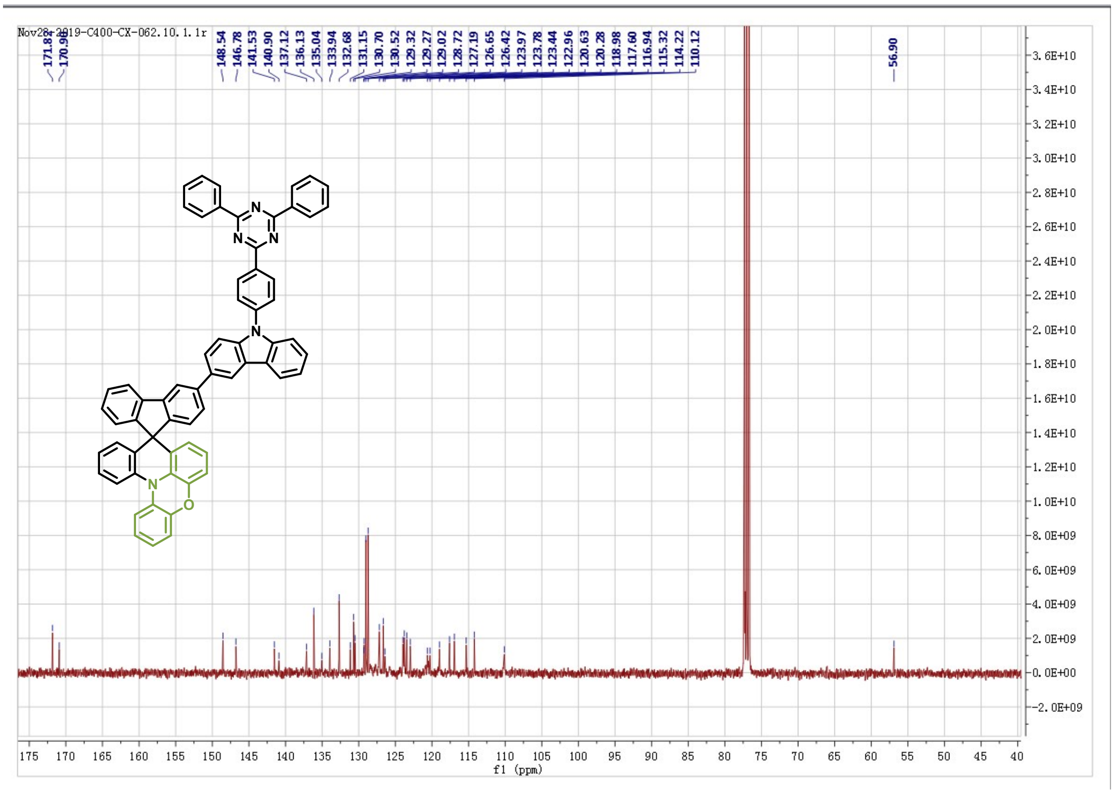

**Figure S4.** 101 MHz $^{13}C$ NMR spectrum of **SFCCNO** measured in $CDCl_3$**.**

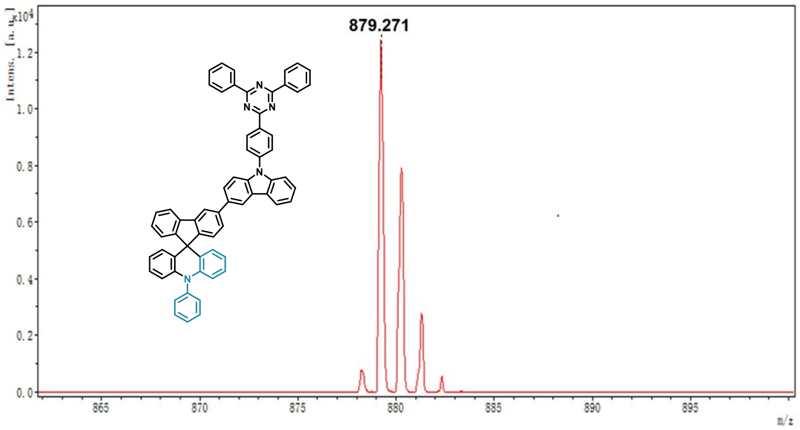

**Figure S5**. MALDI-TOF spectrum of **SFCCN**.

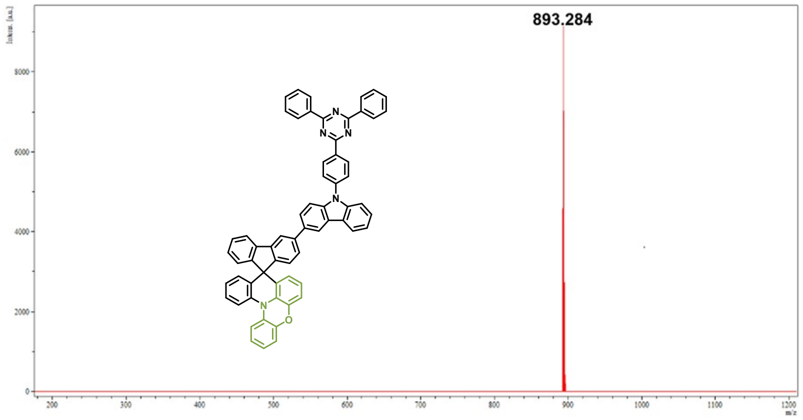

**Figure S6**. MALDI-TOF spectrum of **SFCCNO**.

## 2.2 Thermal properties

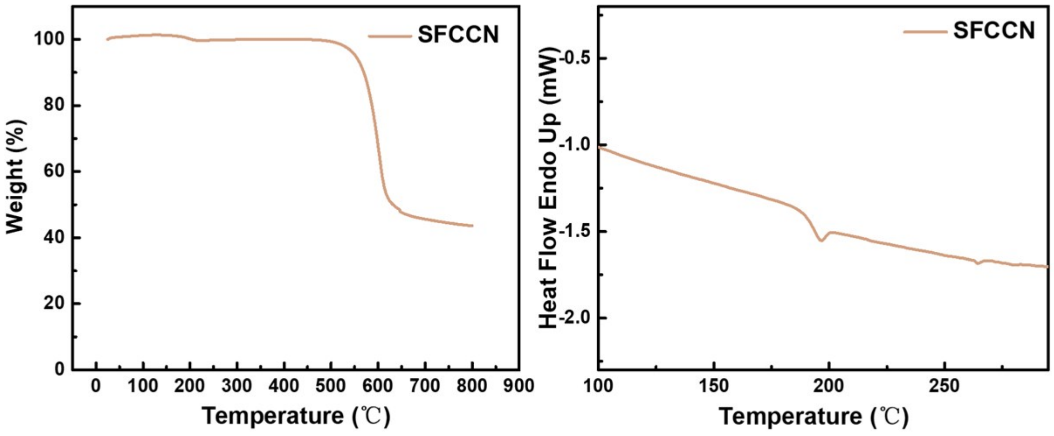

**Figure S7**. Thermal gravimetric analysis (TGA) curve and differential scanning calorimeter (DSC) curve of **SFCCN**.

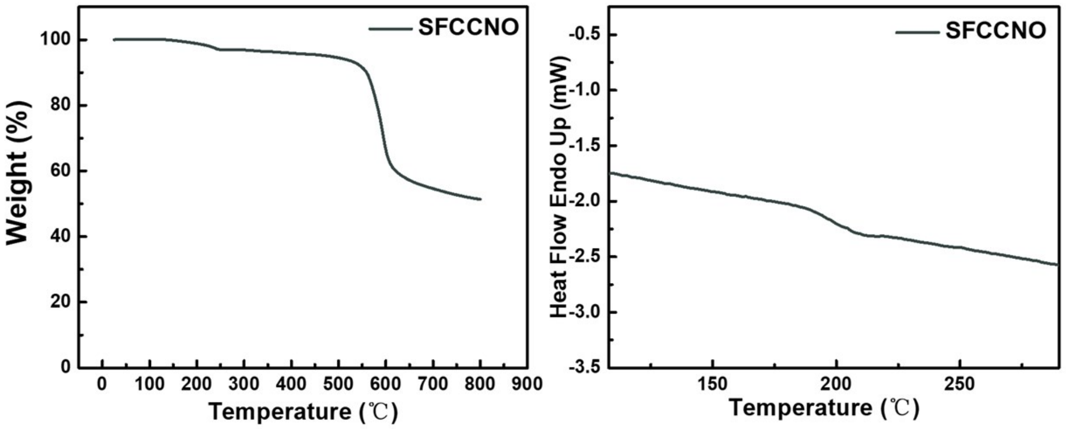

**Figure S8**. Thermal gravimetric analysis (TGA) curve and differential scanning calorimeter (DSC) curve of **SFCCNO**.

### 2.3 Photophysical properties

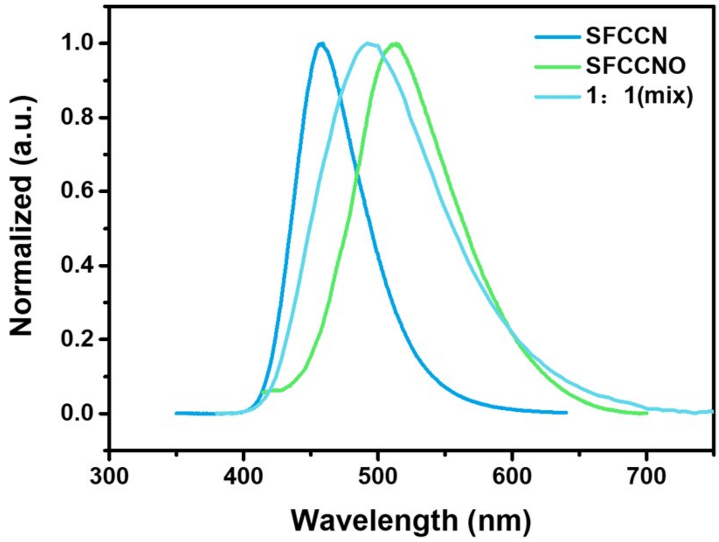

**Figure S9**. The neat film fluorescence spectra of **SFCCN**, **SFCCNO** and **SFCCN: SFCCNO** (mix)

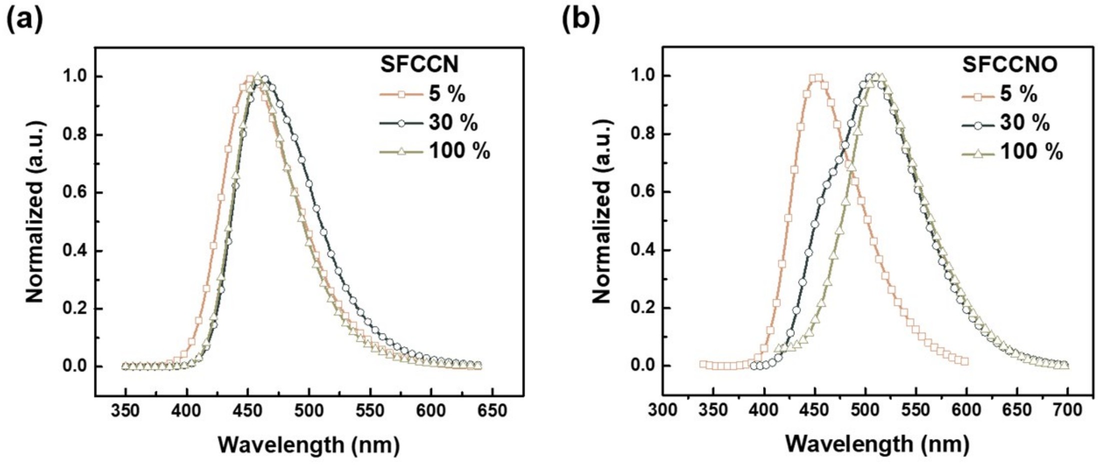

**Figure S10**. Fluorescence spectra of (a) DPEPO: **SFCCN** and (b) DPEPO: **SFCCNO** in film state.

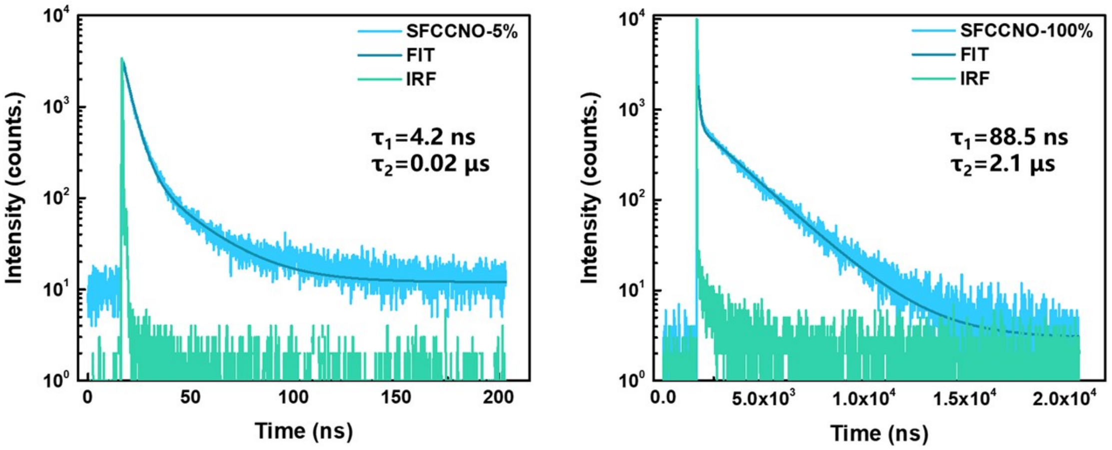

**Figure S11.** Transient photoluminescence spectra of DPEPO: **SFCCNO** (5 wt %) and pristine **SFCCNO** in film state.

## 2.4 Electrochemical properties

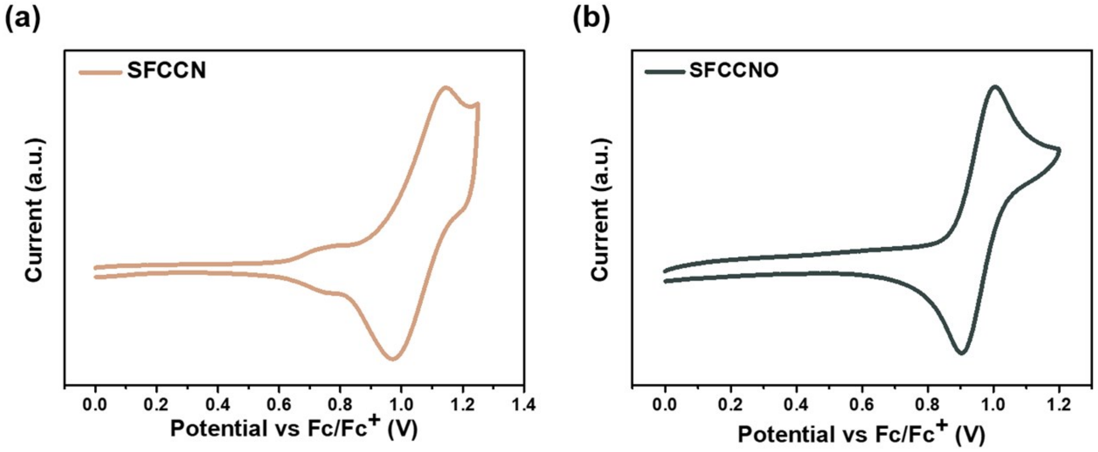

**Figure S12**. Cyclic voltammogram of the **SFCCN** and **SFCCNO**.

## 2.5 DFT data

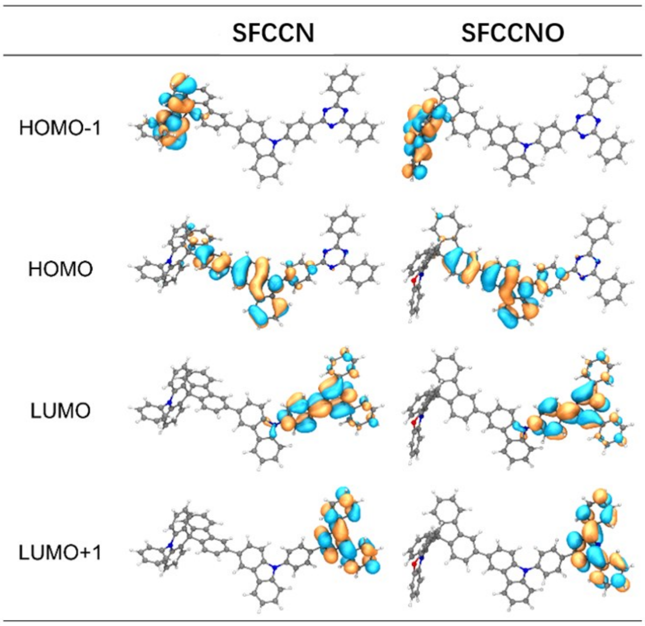

**Figure S13**. Frontier orbital distributions of **SFCCN** and **SFCCNO**.

## 2.6 EL spectra

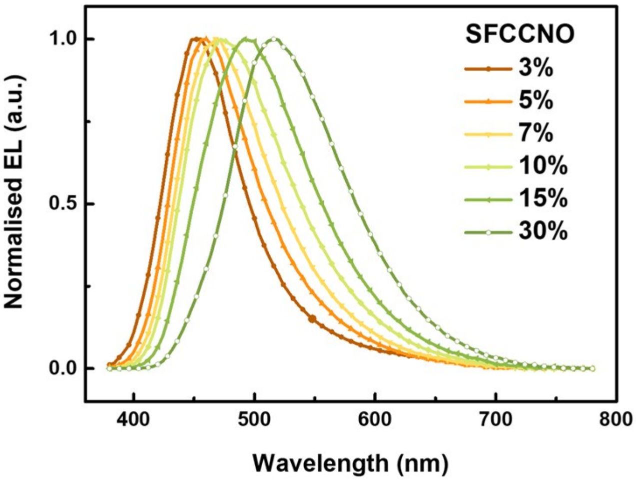

**Figure S14.** EL spectra of DPEPO: **SFCCNO** in film state.

# 3. Supporting Tables

## 3.1 DFT data

**Table S1.** Calculated properties of adiabatic $S_1$ and $T_1$ states and $\Delta E_{\mathrm{ST}}$.

| | $S_1$ | | | $T_1$ | | $\Delta E_{\mathrm{ST}}$ (eV) |
|---|---|---|---|---|---|---|
| | $\lambda$ (nm) | $f$ | orbitals | $\lambda$ (nm) | orbitals | |
| SFCCN | 451.89 | 0.3729 | H1-L:0.963 | 549.51 | H1-L:0.576 | 0.44 |
| SFCCNO | 458.07 | 0.0991 | H1-L:0.957 | 549.89 | H1-L:0.591 | 0.40 |
| SFCCNO dimer | 654.91 | 0.003 | H-L:0.997 | 666.05 | H-L:0.989 | 0.05 |

**Table S2** Calculated frontier orbital levels of **SFCCN** and **SFCCNO** in their ground state

| | HOMO-1 | HOMO | LUMO | LUMO+1 |
|---|---|---|---|---|
| SFCCN | -5.716 | -5.438 | -2.098 | -2.026 |
| SFCCNO | -5.766 | -5.288 | -2.118 | -2.043 |

**Table S3**. Calculated properties of first three singlet states and triplet states at relaxed $S_1$ and $T_1$ geometries, respectively.

| | $S_1$ | | | | $T_1$ | | |
|---|---|---|---|---|---|---|---|
| | eV | nm | $f$ | Orbitals | eV | nm | Orbitals |
| SFCCN | 2.744 | 451.89 | 0.3729 | H1-L:1.0 | 2.256 | 549.51 | H1-L:0.576 |
| | 2.860 | 433.51 | 0.0000 | H-L:0.94 | 2.752 | 450.59 | H2-L3:0.149 |
| | 3.362 | 368.8 | 0.0001 | H1-L1:0.95 | 2.945 | 420.99 | H-L:0.996 |
| SFCCNO | 2.784 | 445.37 | 0.3991 | H1-L:0.96 | 2.255 | 549.89 | H1-L:0.591 |
| | 2.707 | 458.07 | 0.0070 | H-L:0.95 | 2.756 | 449.85 | H1-L2:0.16 |
| | 3.221 | 384.94 | 0.0000 | H-L1:1.0 | 2.773 | 447.09 | H-L:0.929 |
| dimer | 1.893 | 654.91 | 0.003 | H-L:1.0 | 1.862 | 666.05 | H-L:0.989 |
| | 2.457 | 504.54 | 0.0005 | H-L3:1.0 | 2.439 | 508.32 | H-L3:0.981 |
| | 2.713 | 457.08 | 0.0005 | H-L1:1.0 | 2.517 | 492.62 | H3-L:0.495 |

## 3.2 EL performance

**Table S4.** The EL proprieties with 3-30 wt % doping ratio of **SFCCN** and **SFCCNO**

| | Doping ratio (%) | Peak[a] (nm) | FWMH[a] (nm) | Max CE/ PE/ EQE[b] （cd·A$^{-1}$/ lm·W$^{-1}$/ %） | CIE (*x, y*)[a] |
|---|---|---|---|---|---|
| SFCCNO | 3 | 456 | 75 | 2.5/ 1.2/ 1.9 | (0.17, 0.15) |
| | 5 | 460 | 81 | 4.2/ 1.9/ 2.5 | (0.17, 0.20) |
| | 7 | 468 | 89 | 11.5/ 7.0/ 6.1 | (0.18, 0.23) |
| | 10 | 472 | 102 | 14.0/ 9.4/ 6.5 | (0.20, 0.28) |
| | 15 | 492 | 107 | 26.5/ 19.3/ 10.6 | (0.22, 0.37) |
| | 30 | 516 | 95 | 36.5/ 30.9/ 12.9 | (0.29, 0.48) |
| SFCCN | 5 | 460 | 70 | 4.5/ 2.5/ 3.3 | (0.15,0.15) |
| | 30 | 472 | 74 | 18.5/ 15.1/ 10.0 | (0.16,0.23) |

a. Measured at a driving current density at 5 mA cm$^{-2}$; b. maximum data of current efficiency, power efficiency and external quantum efficiency.

# 4 References

1. G. Stefan, E. Stephan, G. Lars, *J. Comput. Chem.*, 2011, **32**, 1456–1465.
2. L. Tian, F. -W. Chen, *J. Comput. Chem.*, 2012, **33**, 580–92.